Production and Solubility of Ectoine: Biochemical and Molecular Dynamics Simulation Studies

Rezazadeh Mofradnia, Soheil
Department of Chemical Engineering, Faculty of Engineering, North Tehran Branch, Islamic Azad University, Tehran, I.R. IRAN

Ashouri, Reihaneh
Department of Environment, Faculty of Environment and Energy, Science and Research Branch, Islamic Azad University, Tehran, I.R. IRAN

Abtahi, Najmeh
Department of Chemical Science, Faculty of Science & Technology, North Tehran Branch, Islamic Azad University, Tehran, I.R. IRAN

Yazdian, Fatemeh*+
Department of Life Science Engineering, Faculty of New Science & Technology, University of Tehran, Tehran, I.R. IRAN

Rashedi, Hamid
Biotechnology Group, School of Chemical Engineering, College of Engineering, University of Tehran, P.O.Box:11155-4563, Tehran, I.R. IRAN

Sheikhpour, Mojgan
Department of Mycobacteriology and Pulmonary Research, Microbiology Research Center (MRC), Pasteur Institute of Iran, Tehran, I.R. IRAN

Ashrafi, Fatemeh
Department of Chemical Science, Faculty of Science & Technology, Islamic Azad University North Tehran Branch, Tehran, I.R. IRAN

ABSTRACT: *In this study, ectoine is produced by Streptomyces.sp IBRC-M PTCC 10615. Fermentation parameters such as flow regime, gas hold up, mass transfer coefficient, and mixing time were optimized by statistical analysis. Streptomyces. sp produced a maximal ectoine concentration of 270 mmol/kg at optimal conditions of ectoine and L-aspartic acid. Also, the amount of mass transfer, gas hold up, and mixing time were determined 0,41/s ,0.3, and 40 s, respectively. The amount of ectoine was measured by HPLC. Furthermore, Molecular Dynamics (MD) simulation was used for studying the solubility of ectoine in aqueous media. Equilibrium data such as temperature, potential energy, and volume graphs showed that the solubility of ectoine is 25 % more than glycerol. Also, all the achieving graphs from the equilibrium of simulation were confirmed the appropriate structure of the system.*

KEYWORDS: *Ectoine; Streptomyces; Molecular dynamic; Thermodynamic principles*.

***** *To whom correspondence should be addressed.*
+ E-mail: yazdian@ut.ac.ir
1021-9986/2020/6/259--269 11/$/6.01

INTRODUCTION

Ectoines are generally distributed in halotolerant eubacteria and halophilic bacteria. Nevertheless, ectoines typically not only hold osmotic activity, but also, have the capability to protect biomolecules in cells such as proteins, membranes against dehydration and enzymes, drying, freezing and heating [1]. Ectoine (1, 4, 5, 6-tetrahydro-2-methyl-4-pyrimidinecarboxylic acid) is a natural compatible solute, which serves as a protectant in many bacterial cells. At first, ectoine was identified in *Ectothiorhodospira halochloris*, an extremely halophilic phototrophic bacterium. Furthermore, the application of ectoine has been approved in skin care products, cosmetics and other biochemical or medical fields[2–4]. Hence, ectoine produced by *Marinococcus, Halomonas ssp*. and *Streptomyces strain C-2012* have been extensively considered as remarkable candidates for applications associated with molecular biology, agriculture, medicine, pharmacy and food processing[1]. Streptomyces, the largest genus of Actinobacteria, are Gram positive mycelia bacteria that have the ability to survive in unfavorable conditions of environment such as saline soils [5–8]. Bioreactors are considered via a definitely directed circulation flow which can be driven in fluidized or fluid systems through propeller or jet drive and generally in gas-liquid systems by liquid pump or airlift drive[9–11]. In some studies, Ectoine production was done using bioreactors however, none of them considered the hydrodynamic parameters and mass transfer in the bioreactors.

In molecular dynamics simulation, the structure and main properties of the material such as stability, intermolecular penetration, and interactions between phases are better shown [12–14]. Additionally, molecular dynamic simulation can be employed to study the behavior of complex materials in molecular-scale, and is used innumerous branches of science, especially biology and nanotechnology [15–17]. This kind of simulation has been noticed in many sub-disciplines because it can be used to predict the drug effect. Of the most essential studies in the field of medicine are biologic treatments for prevalent cancers, using structures such as liposome and mycelium [18–23]. An example of their application is when the simulations are used to select the best type of alloy for analyzing the wave space [24,25]. In numerous morphological structures [26–28], the effect of material size on thermodynamic parameters and reactivity [29,30] and even the survey of dynamic properties and heat exchangers effects [31,32]were considered using molecular dynamic simulations.

In this study, ectoine is produced by *Streptomyces.sp* IBRC-M PTCC 10615. Optimization calculations of the fermentation parameters such as flow regime, gas hold up, mass transfer coefficient and mixing time were carried out. Moreover, molecular dynamic simulation systems were created in Visual Molecular Dynamics (VMD) to compare the water-glycerol and water-ectoine models. The activity of ectoine as a suitable structure was investigated in comparison to glycerol, by analyzing the results of temperature, potential energy, kinetic and volume graphs.

EXPERIMENTAL SECTION

Bacterial strains and culture conditions

Streptomyces. Sp, an ectoine-producing strain was purchased from the Persian type culture collection. Fermentation medium ISP II was used for the preparation of *Streptomyces. sp* seeding material (g/l): malte extract 10, yeast extract 4, sucrose 4, agar 18 [33].

The seeding material was prepared by inoculation of *Streptomyces. sp* at 37 ^{o}C for 6 days. The fermentation flasks were incubated at 37 ^{o}C for 6 days at 150 rpm. Biomass production was measured by the cell dry weight (CDW) method And the Ectoine concentration was measured by HPLC.

Hydrodynamic and mass transfer coefficients

The flow regime was assayed by the fermentation medium, for the prediction of flow patterns of the gas-liquid flow. The gas bubble flow in the vessel was photographed with Canon PowerShot S3 IS which is a high-speed camera[34–39]. The essential time for recognizing a specific percentage of concentration homogeneity is defined by the mixing time(t_m) [39]. Tracer methods were used to calculate the mixing time. This technique is based on measuring the time needed for the decay of a pulse of a tracer (a dye) that is added to various aeration flows [37,40–46]. In this research, Brilliant Blue G (λ = 595 nm) at a total concentration of 0.5mg/l was added to the bioreactor containing 6L of fermentation medium. A spectrophotometer (PG instruments T60 American) was used for recording the amounts of optical density. The repetition of each experiment was performed

in triplicates. Gas hold up (ε) and k_La_{O2} were defined *via* the dynamic gassing out quantity and the suitable techniques of measuring the volume expansion, respectively[37,47,48]. The mass balance of DO in the bioreactor gives Eq. (1) [48]:

$$dC_L/dt = k_L a\left(C^* - C_L\right) \quad (1)$$

Where C_L is the concentration of DO, the saturated oxygen concentration is C*and t is time [49,50]. Moreover, k_La (oxygen) and ε were determined by changing the values of aeration and agitation.

Experimental design

Optimization of ectoine production in the bioreactor was carried out via the design expert software 7. This method was used for finding the relationship between the variables and for obtain their optimum amounts. Thus, ectoine (A) and L-aspartic acid (B) were carefully chosen as efficient parameters. Then, 13 experimental runs through three-level central composite design (CCD) were carried out [51,52].

Molecular dynamic simulation

The aim of the simulation is the investigation of ectoine solubility in comparison to glycerol. All steps of simulation were carried out according to basic thermodynamic principles and main parameters. Furthermore, the production of ectoine was evaluated in the experimental phase and the solvability of ectoine in water was investigated using the MD software.

Computational method

First of all, PDB and the protein file of ectoine were downloaded from PubChem (ID: 126041) and RCSB (DOI: 10.2210/pdb5svz/pdb), respectively. Oligomer glycerol was built via the Material Studio software. The structures were optimized for achieving the stable conformation of them. For optimization of the represented structures with this simulation software, compass ||| as a powerful force field with conformer module was used. In various fields, the application of force field compass ||| was considered. The structure of detergents and drug delivery are the important fields of compass ||| equation. The tertiary structures of glycerol PDB were minimized (steepest descent steps: 1000 by step size). Also, the crystal of glycerol was downloaded in RCSB (DOI: 10.2210/pdb1ldi/pdb). Finally, the minimum controller value at constant temperature (ki) having the lowest binding energy and frequent cluster were investigated. For each of the simulation boxes, a RMS ligand was designed for starting the conformation of the molecular dynamic.

Molecular dynamic

The complex of ectoine and glycerol were centered in a cubic box water (triple point charge: TIP3P immersed *via* the periodic boundary conditions having the distance of 10 Angstrom (Å) from each side of the wall. Sodium chloride (NaCl) was used to neutralize the negative charges present n the aqueous media. The electrostatic interactions were calculated by the Particle Mesh Ewald (PME) technique. A cut-off of 10 Å was applied to Lennard-Jones interactions. During 10,000 steepest-descent, the coupling of algorithm was used for maintaining a constant temperature and pressure for simulations of various components [53] for minimization of energy steps. Thus, position-constrained molecular dynamics (MD) were simulated under isothermal-isobaric (NVT) ensemble for 500 ps. Eventually, the result of simulation were studied under the canonical isothermal-isochoric (NPT) ensemble via NAMD 1.2.9 version [54–56] with the time step of 30000 ps. For simulation of ectoine, CHARMM General Force Field (CGenFF) was employed [57]. The CHARMM General Force Field (CGenFF) covers a wide range of chemical groups present in biomolecules and drug-like molecules, including a large number of heterocyclic scaffolds. The parameterization philosophy behind the force field focuses on quality at the expense of transferability, with the implementation concentrating on an extensible force field. CHARMM force field is the best choice for molecular rotating calculation of macro molecules such as ectoine. Therefore, the freedom of the molecular movement in the simulation box was proved by applying this force field in the steps of the molecular dynamic [58]. The VMD software was used for visualizing the trajectories of structures and their analysis, which include the volume and kinetic energies, energy potential per sections and temperature graphs [59].

RESULTS AND DISCUSSION

Hydrodynamic parameters and mass transfer coefficients (k_La)

The results of various aeration and agitation rates on flow regimes of fermentation medium for ectoine production were investigated. The bubbly (homogeneous) flow regime was considered with the equal radial

scattering of bubbles size. The slug and bubbly types are two flow regimes, which were found according to some bubbles moving at high aerations in the presence of the number of small. It was found that the slug flow regime was seen when the gas flow rate increased to 0.17vvm and the diameter of bubble is 0.3mm in optimal conditions. In addition, in the fermentation medium, the evaluation results of the mixing time in various aerations were considered. By increasing the aeration, the mixing time was decreased. However, no significant effect is observed when the aeration was reduced. Hence, in the optimum conditions, the mixing time reached to 40s [45].

The effects of various aerations on the gas hold up in the bioreactor were also investigated. The gas hold up was enhanced by increasing aeration. However, their correlation was not significant at higher gas flow rates. In all aeration regimes, the gas holds up was improved by increasing the liquid velocity inside the vessel. In addition, the optimized amount of gas hold up was 0.3. Furthermore, at optimal conditions, the mass transfer in the fermentation medium for ectoine production was 0.41/s.

Optimization of parameters for ectoine production

The effect of L- aspartic acid and ectoine on the growth of *Streptomyces. sp* IBRC-M PTCC 10615 were investigated. The maximum production of biomass and ectoine were obtained at 150 rpm. The goal of conducting fermentation in flasks is to maximize ectoine production. The number of regression coefficients were calculated and the fitted equation (2) (in terms of coded values) for the prediction of the production of ectoine (Y) was as follows ($R^2 = 0.89$):

$$Y = 77.5 + 47.50A - 19.50B + 136A^2 \quad (2)$$

Where A and B are ectoine and L-aspartic acid values, respectively. The importance of each coefficient, demonstrated with p-values, is also given in this table.

In this study, the value of the determination coefficient (R^2 =0.89) shows that the variability of response could be described with the model. The differentiation of the quadratic model was used for obtaining the optimal values of the variables for achieving maximum production of ectoine. The predicted optimum production of ectoine corresponding to these values is about 270 mmol/kg. To confirm the model accuracy for predicting the maximum value of ectoine production, additional experiments

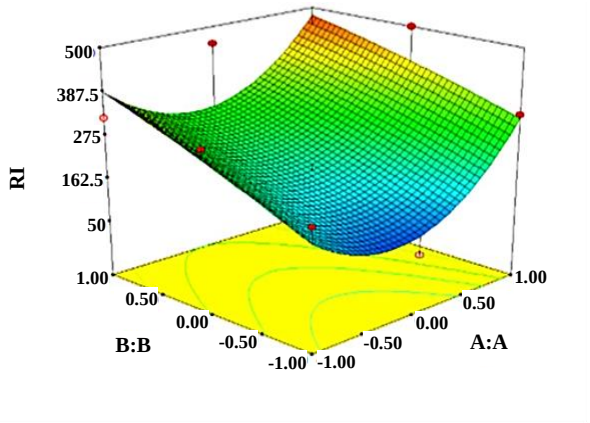

Fig. 1: Contour plot for ectoine production.

in triplicates using the optimized essential aspects were carried out. The experimentally determined production of ectoine at optimal conditions was 281 mmol/kg (281 g/L), which were confirmed by the model's prediction. The graphical representation of the regression equation is the 3D contour plots which are planned to demonstrate the interaction of the variables. The plots of elliptical contour determine that the interaction is essential for the enhancement of optimum production of ectoine.

The entire relationships between factors and responses can be better realized via examining the planned series of contour plots (Fig. 1) generated from the predicted models (Eq. 2). As presented in Fig. 1, the contour plot of responses for ectoine production is 281 mmol/kg at optimum conditions. Other studies presented at the optimal conditions, *Halomonas elongata*, and *Halomonas salina* BCRC 17875 produced 16 g/L ,and 14g/L biomass and ectoine, respectively [1,2]. The ectoine genes *ect* ABC from the halophilic bacterium *Halomonas elongata* were successfully introduced into Escherichia coli K-12 strain BW25113 under the arabinose-inducible promoter. To our delight, a large amount of ectoine was synthesized and excreted into the medium during the course of whole-cell bio catalysis, using aspartate and glycerol as the direct substrates. At low cell density of 5 OD/mL in the flask, under the optimal conditions (100 mM sodium phosphate buffer (pH 7.0), 100 mM sodium aspartate, 100 mM KCl and 100 mM glycerol), the concentration of extracellular ectoine was increased to 2.67 mg/mL. At the high cell density of 20 OD/mL in the fermenter, a maximum titer of 25.1 g/L ectoine was achieved in 24 h [60]. The researchers, To understand the mechanisms of ectoine-

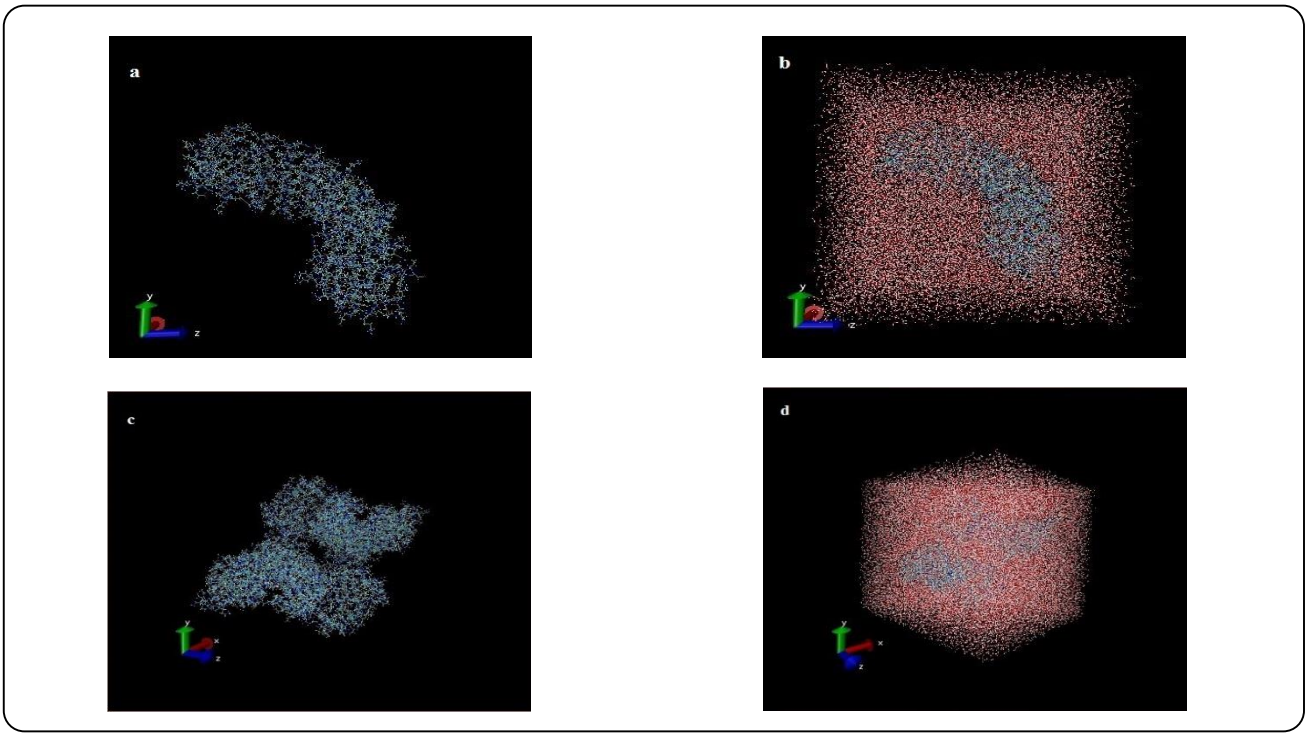

Fig. 2: a) The final Atomistic models of ectoine. b) Visualization of the structural changes induced in ectoine chains due to the inclusion of water. c) Snapshot of the final Atomistic models of glycerol. d) Visualization of the structural changes induced in glycerol chains due to the inclusion of water.

induced osmoprotection in Sinorhizobium meliloti, a proteomic examination of S. meliloti cells grown in minimal medium supplemented with ectoine was undertaken. This revealed the induction of 10 proteins. The protein products of eight genes were identified by using matrix assisted laser desorption ionization–time-of-flight mass spectrometry [61].

Simulation results

In this research, two simulation boxes were created which contain molecules of water, ectoine and glycerol. Hence, the interactions of compounds were simulated via the VMD molecular dynamic software. As presented in Fig. 2, the molecules of ectoine and glycerol were shown. According to the molecular dynamic calculations, a number of diagrams from various variables were achieved such as pressure, temperature, volume, potential and kinetic energy. Analysis of charts showed that the amount of ectoine production in the aqueous media significantly depends on various variables. For investigation of solubility and volume variation, three essential parameters such as temperature, potential and kinetic energy were studied. For evaluation of the reactivity and the stability of the system, the equilibrium and regularity of the system and reactivity of ectoine in the intended temperature were demonstrated via the potential, kinetic energy and temperature, respectively. The obtained result diagrams show the changes of compounds individually in a given time interval.

Temperature analysis

Temperature is an essential factor in all steps of the simulation process. The solvability of glycerol and ectoine molecules were investigated at ambient temperature as a constant intended temperature. Moreover, the parameter of temperature must be changed with 10-grade intervals of temperatures. The changes in temperature would continue until the equilibrium is reached. Equilibrium is due to the sustainability of the reactive structure and the ability of the structure to react rapidly with the system. As presented in Fig. 3a, the peaks of interaction between ectoine and water increase with a gradual slope with a rational rhythm after 5000 time steps at ambient temperature (298 K). Eventually, the reactions were balanced in a temperature of 294 K and the oscillations around this temperature continued until 30,000 versus time steps (vs TS).

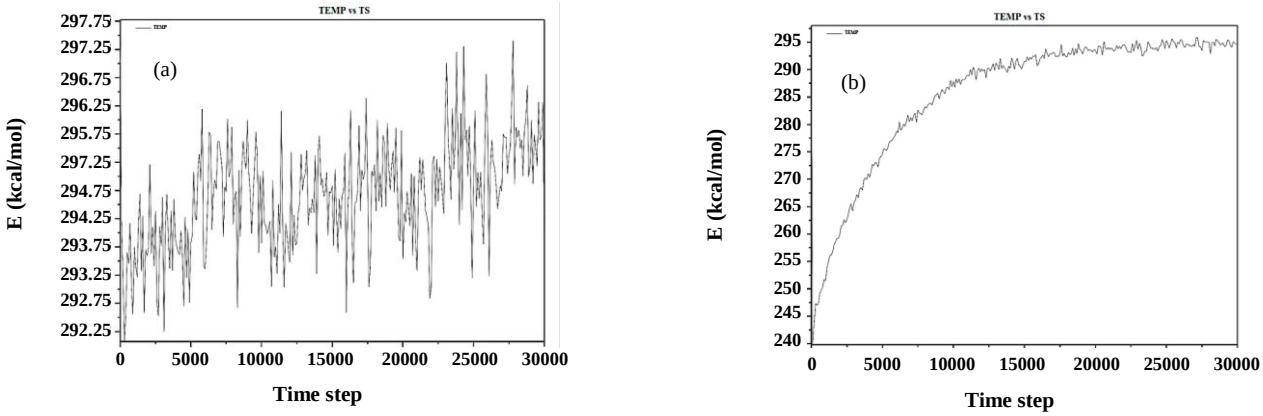

Fig. 3: a) Temperature variation of ectoine. b) Temperature variation of glycerol.

In addition, as shown in Fig. 3b, the input temperature for simulation box of glycerol is 298 K but the beginning of energy production in the system starts at 240 K. Therefore, the peaks of the glycerol graph were gradually increased until 298 K due to the insolubility in water, and latterly to reach equilibrium of glycerol at the intended temperature.

Rezazadeh et al., (2018), investigated the efficacy of Fe/starch nanostructures for increasing the production of biosurfactant. They demonstrated that the controlling of temperature is an essential step in the MD simulation system. Nose-Hoover thermostat controlled each part of the simulation [62]. Furthermore, the high initial peak on the temperature graph was indicated by a high-energy reaction.

Potential energy variations

One of the important parameters for analysis of reactivity in the simulation system is the potential energy. The lower potential energy, the higher capability of structures and system. Moreover, variation of 1000 Kcal/mol energy in a small time interval can be ideal and logical to be explained as potential energy. Hence, ascending or descending oscillation for more than 1000 Kcal/mol results in the destruction and disintegrating of the structure. The potential energy of ectoine was presented in Fig. 6a. The amount of potential energy reached to 180500 Kcal/mol by enhancing 1000 Kcal/mol of energy after 2500 ps. The logical rhythm of fluctuations continues (100 Kcal/mol; descending of potential energy) which shows the ideal conditions. Likewise, the potential graph of glycerol was balanced after 18000 ps as shown in Fig. 6b. The amount of energy increased until 27000 Kcal/mol demonstrated inappropriate conditions. Therefore, rapid reactivity time is an important factor for required solvents in various detergents. ones positive abilities of ectoine is the rapid reactivity time in comparison to glycerol. Rezazadeh et al. (2018) reported that the energy graphs could be organized by two significant factors, stability and interaction between compounds of systems. The results confirmed that by adding nanoparticles, the production of biosurfactant were increased. Likewise, the value of energy was increased by the ability of zero valent iron nanostructure [62]. Other researchers investigated the core-shell of CNT and NanoWire (NW) platinum via molecular dynamic. The results of the total potential energy displayed a considerable downward trend in the first time step (125 ps) then the slope of graph suddenly descended. In contrast to the decreasing of energy, stability and equilibrium of system (CNT–NW) were achieved due to the regular increasing of contact areas between the CNT and nanowire platinum [63].

Kinetic Results

Kinetic energy is investigated to study the equilibrium and regularity of system. The relationship between the variation of temperature and energy are direct. Hence, the more regular temperature changes in the system are dependent on the more reactivity and equilibrium of kinetic energy. By comparing the diagrams of Fig.5 a and b, it is observed that the ascending slope of glycerol was increased until 10000 Kcal/mol, which shows the instability and illogical enhancement of kinetic energy.

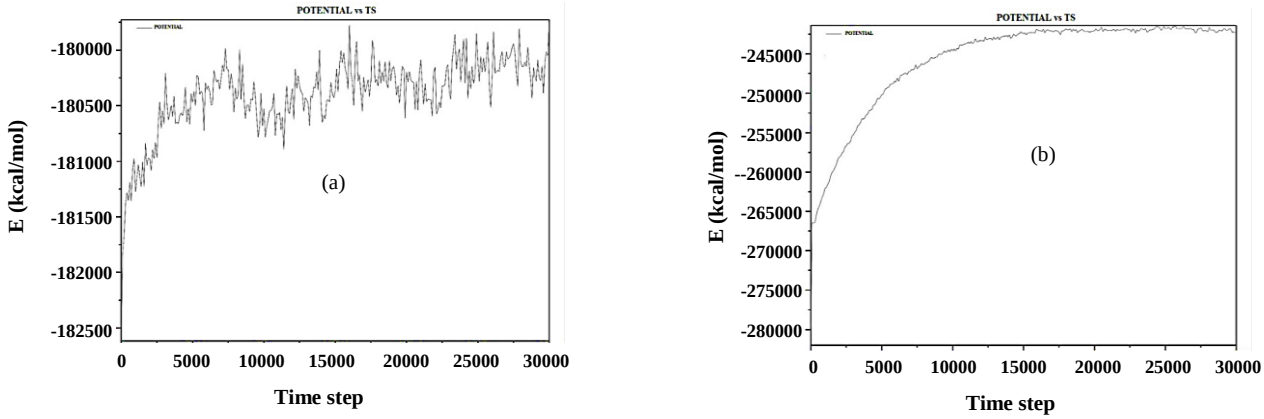

Fig. 4: a) Potential variations of ectoine vs time step. b) Potential variations of glycerol vs time step.

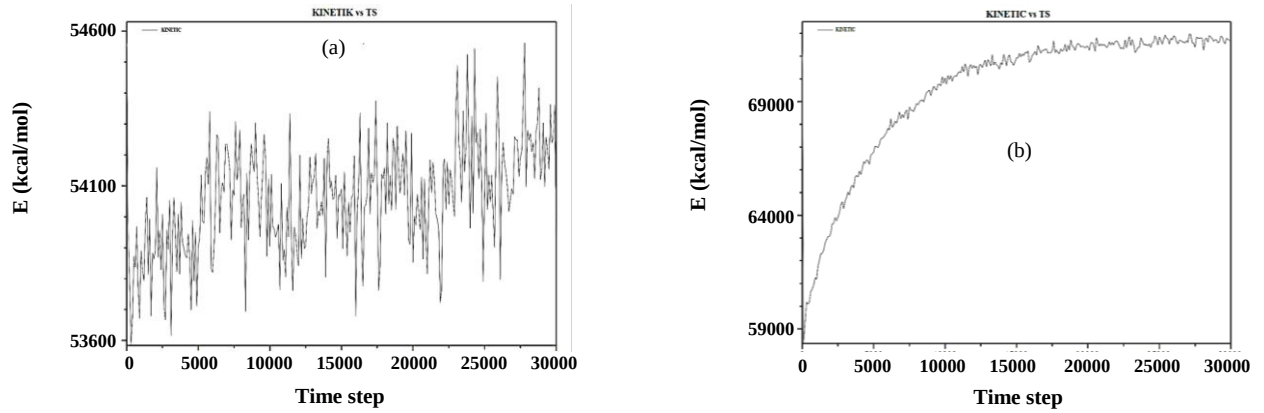

Fig. 5: a) Variations of ectoine kinetic energy vs TS. b) Variations of glycerol kinetic energy vs TS.

Likewise, the ectoine graph demonstrated the stability and reactivity of the system as a purpose of kinetic energy due to enhancement of 4000 Kcal/ mol energy descend within 50000ps. In addition, the more positive value of kinetic energy would be more reliable and acceptable. *Mortazavifar et al.* (2018) predicted the drug delivery and adsorption of carmustine on the surface of boron nitride nanotube via MD simulation. the results showed enhancement in the number of contacts between the two measured fragments, and the energy and stability of the system significantly decrease throughout the adsorption process [63].

Volume analysis of ectoine

As mentioned in the results of temperature, potential and kinetic graphs, the structure of ectoine demonstrates a more environmental and systemic sustainability in comparison to the glycerol molecule. Therefore, decreasing the volume of the ectoine structure would result in more solvability and reactivity of ectoine in the water. Also, all the achieved graphs from the equilibrium of simulation confirmed the appropriate structure of the system. According to Fig. 6a, the volume diagram for ectoine initially increased, up to 5000ps time steps. After thorough analysis of decreasing the volume of ectoine, higher solvability was detected in 3000 time steps. Also, the high hydrophobicity and solubility of ectoine in water is shown in Fig. 6a, where the structural size of ectoine was decreased within the time steps. As a result, the volume changes of ectoine reached from 2.845e+006 angstrom to 2.825e+006 angstrom in comparison to the control diagram. The volume graph of glycerol presented low volume changes, approximately 0.2 angstrom. Eventually, the higher solubility and reactivity of ectoine than glycerol in the aqueous media was approved via MD.

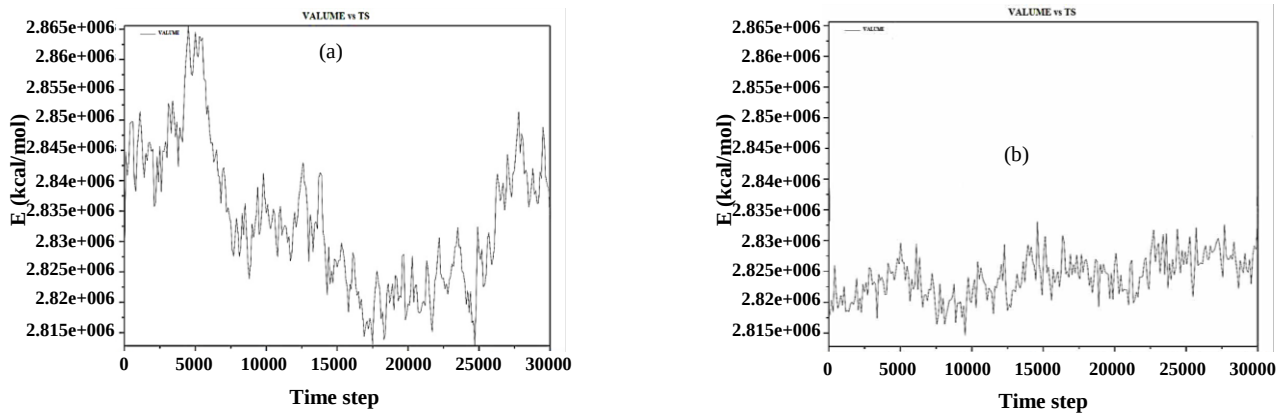

Fig. 6: a) Volume diagram of ectoine versus time. b) Volume diagram of glycerol versus time.

CONCLUSIONS

Ectoine is a natural metabolite matrial that acts as a protective material for the survival of organisms under extreme osmotic stress. *Streptomyces.sp* IBRC-M PTCC 10615 produced ectoine as a natural material metabilic in the fermentation broth. The aerobic bacteria, Streptomyces. sp was grown by batch fermentation using a bioreactor at the temperature of 37°C for a period of 6 days. Statistical analysis was used for optimization of the essential parameters such as the mass transfer coefficient, gas hold up and mixing time which were 0,41/s and 0.3,40 s, respectively. Moreover, Molecular Dynamics (MD) simulation was empolyed for evaluating the solubility of ectoine in comparison to glycerol in the aqueous media. The resulting graphs such as temperature, potential energy and volume graphs demonstrated that the solubility of ectoine is 25% more than glycerol. Therefore, the extrication of energy and temperature is due to exothermicity of the ectoine reaction in the aqueous media.

Acknowledgments

The author announces that this work relies on the thesis research for achieving a master's degree. Moreover, we gratefully acknowledge the department of chemical engineering, faculty of technology and engineering, Faculty of New Science & Technologies, University of Tehran, and research chancellor of the Islamic Azad University, North Tehran Branch for supporting this work.

Received : May 5, 2019 ; Accepted :Aug.26, 2019

REFERENCES

[1] Chen R., Zhu L., Lv L., Yao S., Li B., Qian J., Optimization of the Extraction and Purification of The Compatible Solute Ectoine From Halomonas Elongate in the Laboratory Experiment of a Commercial Production Project, *World J. Microbiol. Biotechnol.*, **33**: 116- (2017).

[2] Chen W.-C., Hsu C.-C., Lan J.C.-W., Chang Y.-K., Wang L.-F., Wei Y.-H., Production and Characterization of Ectoine Using a Moderately Halophilic Strain Halomonas Salina BCRC17875, *J. Biosci. Bioeng.*, : - (2018).

[3] Tavakoli Z., Yazdian F., Tabandeh F., Sheikhpour M., Regenerative Medicine as a Novel Strategy for AMD Treatment: A Review, *Biomed. Phys. Eng. Express*, : - (2019).

[4] Tavakoli Z., Rasekh B., Yazdian F., Maghsoudi A., Soleimani M., Mohammadnejad J., One-Step Separation of the Recombinant Protein by Using the Amine-Functionalized Magnetic Mesoporous Silica Nanoparticles; An Efficient and Facile Approach, *Int. J. Biol. Macromol.*, **135**: 600–608 (2019).

[5] Sadeghi A., Soltani B.M., Jouzani G.S., Karimi E., Nekouei M.K., Sadeghizadeh M., Taxonomic Study of a Salt Tolerant Streptomyces Sp. Strain C-2012 and the Effect of Salt and Ectoine on Lon Expression Level, *Microbiol. Res.*, **169**: 232–238 (2014).

[6] Ghaemi A., Abdi K., Javadi S., Shehneh M.Z., Yazdian F., Omid, M., Rashedi H., Haghiralsadat B.F., Asayeshnaein, O., Novel Microfluidic Graphene Oxide–Protein Amperometric Biosensor for Detecting Sulfur Compounds, *Biotechnol. Appl. Biochem.*, (2019).

[7] Malekimusavi H., Ghaemi A., Masoudi G., Chogan F., Rashedi H., Yazdian F., Omidi M., Javadi S., Haghiralsadat B.F., Teimouri M., Graphene Oxide-L-Arginine Nano-Gel: A Ph-Sensitive Fluorouracil Nanocarrier, *Biotechnol. Appl. Biochem.*, : - (2019).

[8] Bavandi R., Emtyazjoo M., Saravi H.N., Yazdian F., Sheikhpour M., Study of Capability of Nanostructured Zero-Valent Iron and Graphene Oxide for Bioremoval of Trinitrophenol from Wastewater in a Bubble Column Bioreactor, *Electron. J. Biotechnol.*, **39**: 8–14 (2019).

[9] Amoabediny G., Rezvani M., Rashedi H., Jokari S., Chamanrokh P., Mazaheri M., Ghavami M., Yazdian F., Application of a Novel Method for Optimization of Bioemulsan Production in a Miniaturized Bioreactor, *Bioresour. Technol.*, **101**: 9758–9764 (2010).

[10] Khosravi Darani K., Yazdian F., Rashedi H., Madadian Bozorg N., Moradi M., Rezazadeh Mofradnia S., Koller M., Simulation of Bioreactors for PHB Production from Natural Gas, *Iran. J. Chem. Chem. Eng. (IJCCE)*, **39(1)**: 313-330 (2018).

[11] Ashouri R., Ghasemipoor P., Rasekh B., Yazdian F., Mofradnia S.R.M., Ghasemipoor R.A.P., Yazdian B.R.F., Mofradnia S.R.M., The Effect of ZnO-Based Carbonaceous Materials for Degradation of Benzoic Pollutants: A Review, *Int. J. Environ. Sci. Technol.*, : 1–12 (2018).

[12] Razmimanesh F., Amjad-Iranagh S., Modarress H., Molecular Dynamics Simulation Study of Chitosan And Gemcitabine as a Drug Delivery System, *J. Mol. Model.*, **21**: - (2015).

[13] Subashini M., Devarajan P.V., Sonavane G.S., Doble M., Molecular Dynamics Simulation of Drug Uptake by Polymer, *J. Mol. Model.*, **17**: 1141–1147 (2011).

[14] Sahebnazar Z., Mowla D., Karimi G., Yazdian F., Zero-Valent Iron Nanoparticles Assisted Purification of Rhamnolipid for Oil Recovery Improvement from Oily Sludge. *J. Environ. Chem. Eng.*, **6**: 917–922 (2017).

[1] Rungnim C., Rungrotmongkol T., Hannongbua S., Okumura, H., Replica Exchange Molecular Dynamics Simulation of Chitosan for Drug Delivery System Based on Carbon Nanotube, *J. Mol. Graph. Model.*, **39**: 183–192 (2013).

[16] Alamdar N., Rasekh B., Yazdian F., Effects of Fe/SDS and Au Nanoparticles on Pseudomonas Aeroginosa Bacterial Growth and Biosurfactant Production, *IET Nanobiotechnology*, : 26–28 (2018).

[17] Rajab Beigy M., Rasekh B., Yazdian F., Aminzadeh B., Shekarriz M., High Nitrate Removal by Starch-Stabilized FeO Nanoparticles in Aqueous Solution in a Controlled System, *Eng. Life Sci.*, **18**: 187–195 (2018).

[18] Loverde S.M., Klein M.L., Discher D.E., Nanoparticle Shape Improves Delivery: Rational Coarse Grain Molecular Dynamics (rCG-MD) of Taxol in Worm-Like PEG-PCL Micelles, *Adv. Mater.*, **24**: 3823–3830 (2012).

[19] Nash, D., Petrillo, B., Senkl, D., Optimizing the Preparation, Analysis and Formulation of Liposomes for Drug Delivery Applications, *Biophys. J.*, **112**: 580a- (2017).

[20] Alonso H., Bliznyuk A.A., Gready J.E., Combining Docking and Molecular Dynamic Simulations in Drug Design, *Med. Res. Rev.*, **26**: 531–568 (2006).

[21] Moghadam S., Larson R.G., Assessing the Efficacy of Poly (N-isopropylacrylamide) for Drug Delivery Applications Using Molecular Dynamics Simulations, *Mol. Pharm.*, **14**: 478–491 (2017).

[22] Nadvorny D., Soares-Sobrinho J.L., de La Roca Soares M.F., Ribeiro A.J., Veiga F., Seabra G.M., Molecular Dynamics Simulations Reveal the Influence of Dextran Sulfate in Nanoparticle Formation with Calcium Alginate to Encapsulate Insulin, *J. Biomol. Struct. Dyn.*, : 1–6 (2017).

[23] Khezri A., Karimi A., Yazdian F., Jokar M., Mofradnia S.R., Rashedi H., Tavakoli Z., Molecular Dynamic of Curcumin/Chitosan Interaction Using a Computational Molecular Approach: Emphasis on Biofilm Reduction, *Int. J. Biol. Macromol.*, #pagerange# (2018).

[24] Separdar L., Davatolhagh S., Effect of Gold Nanoparticles on Structure and Dynamics of Binary Lennard-Jones Liquid: Wave-Vector Space Analysis, *Phys. A Stat. Mech. Its Appl.*, **463**: 163–173 (2016).

[25] Foroughi M.M., Elmi S., Dehdab M., Shahidi-Zandi M., Computational Evaluation of Corrosion Inhibition of Four Quinoline Derivatives on Carbon Steel in Aqueous Phase, *Iran. J. Chem. Chem. Eng. (IJCCE)*, **38**: 185–200 (2019).

[26] Wu L., Zhang Y., Wen Y.-H., Zhu Z.-Z., Sun S.-G., Molecular Dynamics Investigation of Structural Evolution of Fcc Fe Nanoparticles under Heating Process, *Chem. Phys. Lett.*, **502**: 207–210 (2011).

[27] Mofradnia S.R., Ashouri R., Tavakoli Z., Shahmoradi F., Rashedi H., Yazdian F., Effect of Zero-Valent Iron/Starch Nanoparticle on Nitrate Removal Using MD Simulation, *Int. J. Biol. Macromol.*, (2018).

[28] Rezapour N., Rasekh B., Mofradnia S.R., Yazdian F., Rashedi H., Tavakoli Z., Molecular Dynamics Studies of Polysaccharide Carrier Based on Starch in Dental Cavities, *Int. J. Biol. Macromol.*, **121**: 616–624 (2018).

[29] Zhao B., Huang J., Bartell L.S., Molecular Dynamics Studies of the Size and Temperature Dependence of The Kinetics of Freezing of Fe Nanoparticles, *J. Solid State Chem.*, **207**: 35–41 (2013).

[30] Safajou Jahankhanemlou M., Salami Kalajahi M., Modeling of Reversible Chain Transfer Catalyzed Polymerization by Moment Equations Method, *Iran. J. Chem. Chem. Eng.(IJCCE)*, **32**: 59–67 (2013).

[31] Das A., Ghosh M.M., MD Simulation-Based Study on the Melting and Thermal Expansion Behaviors of Nanoparticles Under Heat Load, *Comput. Mater. Sci.*, **101**: 88–95 (2015).

[32] Jamal Davoodi, Investigation of Mechanical and Thermal Properties of Cobalt Metal by Molecular Dynamics Simulation, *Iran. J. Phys. Res.*, **11**: 161–166 (1390).

[33] Tafreshi S.H., Mirdamadi S., Norouzian D., Khatami S., Sardari S., Optimization of Non-Nutritional Factors for a Cost-Effective Enhancement of Nisin Production Using Orthogonal Array Method, *Probiotics Antimicrob. Proteins*, **2**: 267–273 (2010).

[34] Brown R.A.S., Govier G.W., High-Speed Photography in the Study of Two-Phase Flow, *Can. J. Chem. Eng.*, **39**: 159–164 (1961).

[35] Bendjaballah N., Dhaouadi H., Poncin S., Midoux N., Hornut J.-M., Wild G., Hydrodynamics and Flow Regimes in External Loop Airlift Reactors, *Chem. Eng. Sci.*, **54**: 5211–5221 (1999).

[36] Panáček A., Kvítek L., Prucek R., Kolář M., Večeřová R., Pizúrová N., Sharma V.K., Nevěčná T., Zbořil R., Silver Colloid Nanoparticles: Synthesis, Characterization, and Their Antibacterial Activity, *J. Phys. Chem. B*, **110**: 16248–16253 (2006).

[37] Yazdian F., Shojaosadati S.A., Nosrati M., Pesaran Hajiabbas M., Malek Khosravi K., On-Line Measurement of Dissolved Methane Concentration During Methane Fermentation in a Loop Bioreactor, *Iran. J. Chem. Chem. Eng. (IJCCE)*, **28**: 85–93 (2009).

[38] Chisti Y., Pneumatically Agitated Bioreactors in Industrial And Environmental Bioprocessing: Hydrodynamics, Hydraulics, and Transport Phenomena, *Appl. Mech. Rev.*, **51**: 33–112 (1998).

[39] Yazdian F., Shojaosadati S.A., Nosrati M., Vasheghani-Farahani E., Mehrnia M.R., Comparison of Different Loop Bioreactors Based on Hydrodynamic Characteristics, Mass Transfer, Energy Consumption and Biomass Production from Natural Gas. *Iran. J. Chem. Chem. Eng. (IJCCE)*, **29**: 37–56 (2010).

[40] Papagianni M., Mattey M., Kristiansen B., Citric acid Production and Morphology of Aspergillus Niger as Functions of the Mixing Intensity in a Stirred Tank and a Tubular Loop Bioreactor, *Biochem. Eng. J.*, **2**: 197–205 (1998).

[41] Verlaan P., Van Eijs A.M.M., Tramper J., Van't Riet K., Luyben K.C.A.M., Estimation of Axial Dispersion in Individual Sections of an Airlift-Loop Reactor, *Chem. Eng. Sci.*, **44**: 1139–1146 (1989).

[42] Fields P.R., Slater N.K.H., Tracer Dispersion in a Laboratory Air-Lift Reactor, *Chem. Eng. Sci.*, **38**: 647–653 (1983).

[43] Merchuk J.C., Yunger R., The Role o the Gas—Liquid Separator of Airlift Reactors in the Mixing Process, *Chem. Eng. Sci.*, **45:** 2973–2975 (1990).

[44] Petrović D.L., POŠ Arac D., Duduković A., Prediction of Mixing Time in Airlift Reactors, *Chem. Eng. Commun.*, **133**: 1–9 (1995).

[45] Gavrilescu M., Tudose R.Z., Mixing Studies in External-Loop Airlift Reactors, *Chem. Eng. J.*, **66**: 97–104 (1997).

[46] Klein P., Lapeyre G., Large W.G., Wind Ringing of the Ocean in Presence of Mesoscale Eddies, *Geophys. Res. Lett.*, **31**: - (2004)

[47] Al Taweel A.M., Yan J., Azizi F., Odedra D., Gomaa H.G., Using in-Line Static Mixers to Intensify Gas–Liquid Mass Transfer Processes, *Chem. Eng. Sci.*, **60**: 6378–6390 (2005).

[48] Chisti Y., Moo-Young M., On the Calculation of Shear Rate and Apparent Viscosity in Airlift and Bubble Column Bioreactors, *Biotechnol. Bioeng.*, **34**: 1391–1392 (1989).

[49] Sheehan B.T., Johnson M.J., Production of Bacterial Cells from Methane, *Appl. Microbiol.*, **21**: 511–515 (1971).

[50] Lamb S.C., Garver J.C., Batch-and Continuous-Culture Studies of a Methane-Utilizing Mixed Culture, *Biotechnol. Bioeng.*, **22**: 2097–2118 (1980).

[51] Irani Z.A., Mehrnia M.R., Yazdian F., Soheily M., Mohebali G., Rasekh B., Analysis of Petroleum Biodesulfurization in an Airlift Bioreactor Using Response Surface Methodology, *Bioresour. Technol.*, **102**: 10585–10591 (2011).

[52] Fatemi S.M., Foroutan M., Molecular Dynamics Simulations of Freezing Behavior of Pure Water and 14% Water-NaCl Mixture Using the Coarse-Grained Model, *Iran. J. Chem. Chem. Eng. (IJCCE)*, **35**: 1–10 (2016).

[53] Cheatham III T.E., Miller J.L., Spector T.I., Cieplak P., Kollman P.A., Molecular Dynamics Simulations on Nucleic Acid Systems Using the Cornell et al. Force Field and Particle Mesh Ewald Electrostatics, in ACS Publications, (1998).

[54] Kalé L., Skeel R., Bhandarkar M., Brunner R., Gursoy A., Krawetz N., Phillips J., Shinozaki A., Varadarajan K., Schulten K., NAMD2: Greater Scalability for Parallel Molecular Dynamics, *J. Comput. Phys.*, **151**: 283–312 (1999).

[55] Phillips J.C., Braun R., Wang W., Gumbart J., Tajkhorshid E., Villa E., Chipot C., Skeel R.D., Kale L., Schulten K., Scalable Molecular Dynamics with NAMD, *J. Comput. Chem.*, **26**: 1781–1802 (2005).

[56] Nose S., Constant-Temperature Molecular Dynamics, *J. Phys. Condens. Matter*, **2**: - (1990)

[57] Zoete V., Cuendet M.A., Grosdidier A., Michielin O., SwissParam: a Fast Force Field Generation Tool for Small Organic Molecules, *J. Comput. Chem.*, **32**: 2359–2368 (2011).

[58] Fritsch D., Koepernik K., Richter M., Eschrig H., Transition Metal Dimers as Potential Molecular Magnets, *J. Comput. Chem.*, **1145**: 2210–2219 (2008).

[59] Humphrey W., Dalke A., Schulten K., VMD: Visual Molecular Dynamics, *J. Mol. Graph.*, **14**: 33–38 (1996).

[60] He Y.Z., Gong J., Yu H.Y., Tao Y., Zhang S., Dong Z.Y., High production of Ectoine from Aspartate and Glycerol by Use of Whole-Cell Biocatalysis in Recombinant Escherichia Coli, *Microb. Cell Fact.*, **14**: 1–10 (2015).

[61] Jebbar M., Sohn-bo L., Bremer E., Blanco C., Ectoine-Induced Proteins in, **187**: 1293–1304 (2005).

[62] Mofradnia S.R., Tavakoli Z., Yazdian F., Rashedi H., Rasekh B., Fe/starch Nanoparticle-Pseudomonas Aeruginosa: Bio-physiochemical and MD Studies, *Int. J. Biol. Macromol.*, pp. #pagerange# (2018).

[63] Zhang D., Liu Z., Yang H., Liu A., Molecular Dynamics Study of Core–Shell Structure from Carbon Nanotube and Platinum Nanowire, *Mol. Simul.*, **7022**: 1–5 (2018).